Proceedings of the 47th International School and Conference on the Physics of Semiconductors "Jaszowiec 2018"

Fermionic Moore–Read Fractional Chern Insulator in the Thin-Torus Limit

B. Jaworowski*, P. Kaczmarkiewicz and A. Wójs
Department of Theoretical Physics, Wrocław University of Science and Technology, Wybrzeże Wyspiańskiego 27, 50-370 Wrocław, Poland

We investigate a fermionic Thouless pump in the Rice–Mele model at half filling of the lower band. Such a system can be regarded as a 1D limit of a 2D flat-band Chern insulator. We consider two kinds of model interaction, a two- and three-body one. We show that both of them lead to the emergence of Moore–Read-like states provided that the energy scale of the interaction is small compared to the band gap. However, when the interaction is stronger, the two types yield different results: while for the latter the Moore–Read-like state is stable, in the former case it is destroyed by the band mixing.

DOI: 10.12693/APhysPolA.134.919
PACS/topics: 73.43.–f, 03.65.Vf

1. Introduction

The topological flat bands (TFBs) are the lattice counterparts of the Landau levels, allowing for the existence of the fractional Chern insulators (FCI), states analogous to the fractional quantum Hall (FQH) liquids [1, 2]. The FQH states can be intuitively understood in terms of the thin-torus (TT) limit [3]. Such an approach was also applied to FCIs [4–8]. In addition to studying the TT limit of Laughlin states [4–6, 8], it was shown that the TT limit of bosonic Moore–Read (MR) and Read–Rezayi states can be created by applying a three- or four-body interaction [7]. Here we show that a fermionic MR TT state emerges in the 1D flat band model with two- or three-body interaction. Although such a state is not topologically ordered *per se*, we consider a setup of a Thouless pump, within which the Chern number can be defined as the system depends on an external parameter.

It is often assumed in the calculations that the energy scale of the interaction, leading to the presence of FCIs, is much smaller than the band gap. However, the Laughlin FCI (both in 2D and in TT limit) was shown to be stable even for infinite interaction — although one could have expected that the band mixing destroys it [9, 10]. Here, we study this issue for the TT MR state and show that it is destroyed by large enough two-body interaction, but remains stable if the interaction is three-body.

2. Model

We work within the Rice–Mele (RM) model [11]. It contains two sites A, B per unit cell (orange and blue circles in Fig. 1a, respectively) and can be described by a Hamiltonian

$$H=\tau_1\sum_n a_n^\dagger b_n+\tau_2\sum_n b_n^\dagger a_{n+1}+\epsilon\sum_n(-a_n^\dagger a_n+b_n^\dagger b_n),$$

where a_n, b_n are the annihilation operators of a particle on site A,B, respectively, in unit cell n. To define a pumping cycle, we introduce a parameter ϕ_y. The hopping integrals vary with ϕ_y with a period of 2π. We divide the hoppings into variable parts t_1, t_2 and a constant part t_c, so that $\tau_{1,2}=t_{1,2}+t_c$. We choose $t_1=0, t_2=\cos(\phi_y)$ for $\phi_y\in[2k\pi-\pi/2, 2k\pi+\pi/2), k\in\mathbb{Z}$ and $t_1=-\cos(\phi_y), t_2=0$ for $\phi_y\in[2k\pi+\pi/2, 2k\pi+3\pi/2), k\in\mathbb{Z}$, as well as $\epsilon=\sin(\phi_y)$ for any ϕ_y (see Fig. 1b–d).

We start from $t_c=0$ case, for which both bands are exactly flat. At each ϕ_y one of the hoppings $\tau_{1,2}$ vanishes, and the model breaks into the set of disconnected dimers. The energy eigenstates of each dimer, created by operators $\gamma_n^\dagger$, $\delta_n^\dagger$, where n labels the dimers, are the Wannier functions (WFs) of lower and upper band, respectively. For the lower band, they are created by operators

$$\gamma_n^\dagger=\begin{cases}\frac{1}{A}(\cos(\phi_y)b_{n-1}^\dagger-(1+\sin(\phi_y))a_n^\dagger), & \phi_y\in[0,\frac{\pi}{2}],\\ \frac{1}{A}((-1-\sin(\phi_y))a_n^\dagger+\cos(\phi_y)b_n^\dagger), & \phi_y\in[\frac{\pi}{2},\pi),\\ \frac{1}{A}(\cos(\phi_y)a_n^\dagger+(1+|\sin(\phi_y)|)b_n^\dagger), & \phi_y\in[\pi,\frac{3\pi}{2}),\\ \frac{1}{A}((1+\sin(\phi_y))b_n^\dagger-\cos(\phi_y)a_{n+1}^\dagger), & \phi_y\in[\frac{3\pi}{2},2\pi].\end{cases}$$

with $A=\sqrt{2+2\sin(\phi_y)}$ being the normalization constant. They exhibit the shift property $\gamma_n(2\pi)=\gamma_{n+1}(0)$ (see Fig. 1e).

When the lowest band is fully filled, the shift property guarantees that in one pumping cycle (ϕ_y changing from 0 to 2π) every particle is transported by one unit cell. Since the pumped charge is proportional to a 1D realization of the Chern number, it does not change when finite t_c is introduced, as long as it does not close the band gap for any value of ϕ_y (which occurs for $t_c=-0.5$).

If ϕ_y is interpreted as momentum in the y direction, the RM model can be thought of as a 1D limit of a 2D flat band model. The shift property of the Wannier functions guarantees that its bands are topologically nontrivial. The hoppings can be deduced from

*corresponding author; e-mail: blazej.jaworowski@pwr.edu.pl

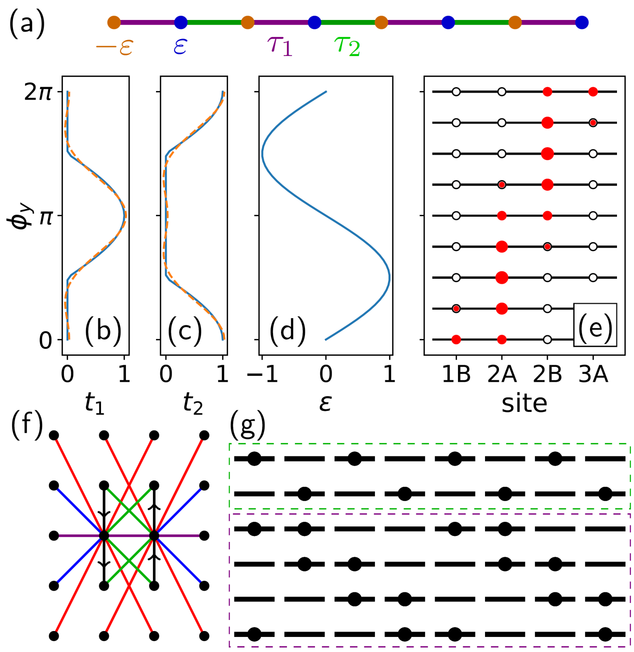

Fig. 1. The topological charge pump in the RM model. (a) The model parameters. The circles and lines denote the sites and hoppings, respectively. (b–d) The dependence of model parameters on ϕ_y in the perfect case (blue solid lines) and in the approximate case with three first Fourier components kept (orange dashed lines). (e) The WF $\gamma_2^\dagger |0\rangle$ for different ϕ_y. The areas of red dots correspond to particle density on given sites (empty circles). (f) The 2D lattice model whose approximate 1D limit is the RM model. The lines correspond to hoppings: $1/\pi$ (violet), $i/2$ (black along arrow), $1/4$ (blue), $-1/4$ (green), $1/(3\pi)$ (red). Only hoppings starting from one unit cell are shown. (g) The six ground states of a many-particle system of a $L = 8$ system with $N_{\rm part} = 4$ particles. The dashes are the WFs, while the circles denote the particles.

the decomposition of τ_1, τ_2 and ϵ into Fourier series in ϕ_y. The maximum flatness is achieved at $t_c = 0$. A strictly flat band requires infinite-range hoppings in the y direction. However, a good approximation can be achieved by considering three first terms of the t_1 and t_2 series (see the orange lines in Fig. 1b,c), which correspond to hoppings up to fourth neighbours (see Fig. 1f) and a bandwidth-to-bandgap ratio (flatness ratio) $F \approx 0.058$.

3. Results

We investigate the many-particle states occurring at half-filling of the lower band of the RM model by studying finite chains of length L unit cells, populated with $N_{\rm part}$ particles, using the exact-diagonalization (ED) and density matrix renormalization group (DMRG) methods. We start from the $t_c = 0$ case. To achieve the MR TT states with a two-body interaction $\hat{V}_{2B}$, we require that after the projection to the lower band, it can be expressed as

$$P\hat{V}_{2B}P = \frac{1}{2}\sum_{m,n} V_{|m-n|}\gamma_m^\dagger\gamma_n^\dagger\gamma_n\gamma_m, \tag{1}$$

where every quantity and operator except from $\hat{V}_{2B}$ depends on ϕ_y, P is the projector to the lowest band, and the coefficients V_i satisfy the equalities $V_3 = V_1/3 = V_2/2$ and $V_{i>3} = 0$ at any ϕ_y. Such an interaction is a fermionic analog of an effective spin Hamiltonian for FQH MR TT states [10], and naturally implements a MR generalized Pauli principle (GPP), leading to the occurrence of 6 degenerate ground states at half-filling [12]. When ϕ_y is varied by 2π, each of the ground states is shifted by one unit cell. Thus, the states return to themselves after four pumping cycles. This results in the pumping of two particles, hence the average charge pumped in one cycle is a half the charge of the single particle. This is a 1D analog of the fractional Hall conductivity. If the filling is slightly lower than 1/2, the number of ground states agrees with the number of quasihole states in GPP.

For Eq. (1) to be valid at any ϕ_y, we introduce a model two-body interaction of the form

$$\hat{V}_{2B} = \frac{1}{2}\sum_{i,j} U_{|i-j|}n_i n_j, \tag{2}$$

where i, j are the site indices (odd and even i correspond to A and B sites, respectively), n_i is the particle density operator at site i, and $U_{|i-j|}$ is a coefficient depending on the distance between sites i and j. We set $U_1 = 4U$, $U_2 = 3U$, $U_3 = 2U$, $U_4 = 2U$, $U_5 = 2U$, $U_1 = U$, and $U_i = 0$ for $i > 6$. In general, we perform the calculations without explicit band projection.

Finite t_c introduces coupling between the dimer wave functions, both within each band and between the bands. This results in lifting of the degeneracy of the six ground states. Unlike the degeneracy splitting of the thin-torus Laughlin states [5, 8], it does not vanish in the thermodynamic limit. This can be understood by treating t_c as a perturbation. Regardless of the system size, the effective Hamiltonian in the perturbation theory has second-order terms, whose value is different for two groups of states enclosed in two dashed boxes in Fig. 1g. The effect of introducing t_c into the $\phi_y = 0$ system with $\hat{V}_{2B}$ and $U = 1$ is seen in Fig. 2a. For both positive and negative t_c we observe the splitting of the six-fold degenerate ground state into two groups containing two and four states. The states within the second group are also split, which is a result of the finite size of the system. For negative t_c the many-particle gap closes at $t_c = -0.5$, which coincides with the single-particle topological phase transition. Although no such transition occurs at positive t_c, the energy splitting of the ground states leads to gap closing at $t_c \approx 1$.

The lifting of the degeneracy of the ground states allows for the observation of the spectral flow, which is one of the signatures of the FCI states which is preserved in the thin torus limit [5, 8]. It can be observed by introducing twisted boundary conditions with the phase $e^{i\phi_x}$ in the x direction. Figure 2b and c shows the evolution of the six lowest energy levels with ϕ_x. The levels di-

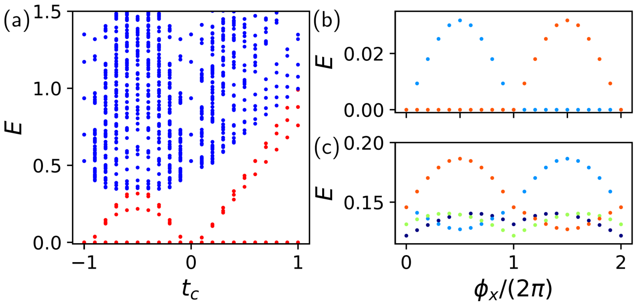

Fig. 2. (a) The ED energy spectrum of a band-projected $L = 12, N_{\mathrm{part}} = 6$ system with $\hat{V}_{2B}$, $U = 1$, at $\phi_y = 0$, as a function of t_c. The six lowest states are shown in red, the rest of states in blue. (b,c) The spectral flow of a $L = 12$, $N_{\mathrm{part}} = 6$, $\phi_y = 0$, $t_c = -0.2$ system for (b) two lowest eigenvalues, (c) four next eigenvalues from six quasi-degenerate ground states. The colors correspond to momenta. All spectra are rescaled so that the ground state is at energy zero.

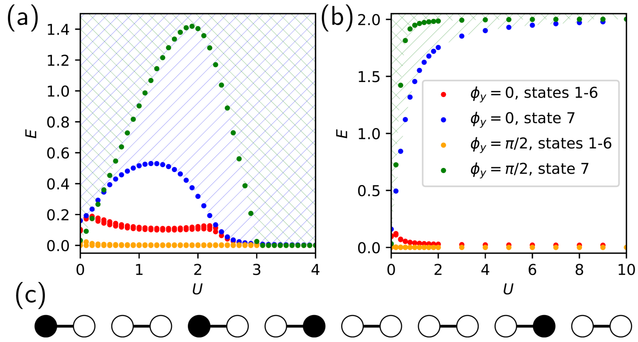

Fig. 3. (a),(b) The low-energy spectrum of the $L = 12$, $N_{\mathrm{part}} = 6$ system with $t_c = 0.2$ as a function of interaction strength: (a) ED results for $\hat{V}_{2B}$, (b) DMRG results for $\hat{V}_{3B}$, obtained using the iTensor software [13]. Seven lowest eigenvalues at $\phi_y = 0$ and $\phi_y = \pi/2$ are shown. The hatching in (a) and (b) symbolizes the fact that we are interested only in the gap between the 6th and 7th state. (c) A site-space configuration of a $L = 8$, $N_{\mathrm{part}} = 4$, $\phi_y = 0$ system yielding lowest interaction energy $E_{int} = 14U$, compared to the energy $E_{int} = 16U$ of the band-projected ground state. Filled and empty circles denote filled and empty sites, respectively, and lines reflect the dimerization of sites.

vide into three pairs, in each of which the states flow into each other as the phase changes by 2π, which is a behavior characteristic to the Moore–Read FCI.

Figure 3 shows the energy spectrum of a $L = 12$ chain with $t_c = 0.2$ as a function of U. Many-body gap above 6th state in (a) closes for sufficiently strong interaction ($U \approx 2.3$), i.e. the MR TT state is destroyed by interband excitations. This can be compared with another way of implementing the GPP — using a three-body interaction

$$\hat{V}_{3B} = U \sum_i \sum_{j=1}^{6} \sum_{k=j}^{6} (n_i n_{i+j} n_{i+k} + n_i n_{i-j} n_{i-k}).$$

Then, the gap closing does not occur (see Fig. 3b). The difference between these two approaches can be easily understood. For $\hat{V}_{2B}$ we can construct a configuration (Fig. 3c) which has lower interaction energy than any of the configuration making up the MR TT states. On the other hand, all the six MR TT states for $\hat{V}_{3B}$ have zero interaction energy. The finite gap for large U can be explained by the fact that in the $U \to \infty$ limit the hopping between the dimers is suppressed and the lowest excitation consists of moving the particle from γ to δ WF within a dimer, which costs energy 2. Indeed, the many-body gap in Fig. 3b seems to converge to 2.

4. Summary and conclusions

In summary, we have shown the emergence of the Moore–Read-like states in the thin torus limit of a fractionally filled topological flat band model. For the perfectly dimerized model and small interaction, we obtained the analytical solutions not only for a 3-body model interaction, but also for a 2-body one. Adding a finite coupling between dimers splits the degeneracy of the sixfold ground state. Unlike the 2D case, the splitting does not have to vanish in the thermodynamic limit, hence it is not a topological degeneracy. This shows that the MR TT states are not topologically ordered, which was expected, as the topological order cannot exist in purely 1D states with conserved particle numbers. It was also shown for the Laughlin FCIs that their 1D counterparts are symmetry-protected phases [4, 6]. We investigated also the influence of the interband excitations on the stability of the MR-like states. We have shown that these states are destroyed when a too strong two-body interaction is applied. However for three-body interaction they survive even when its strength far exceeds the band gap.

Acknowledgments

This work is supported by National Science Centre, Poland (NCN) grant PRELUDIUM no. 2016/21/N/ST3/00843.

References

[1] D.N. Sheng, Zheng-Cheng Gu, Kai Sun, L. Sheng, *Nature Commun.* **2**, 389 (2011).

[2] T. Neupert, L. Santos, C. Chamon, C. Mudry, *Phys. Rev. Lett.* **106**, 236804 (2011).

[3] E.J. Bergholtz, A. Karlhede, *Phys. Rev. B* **77**, 155308 (2008).

[4] B.A. Bernevig, N. Regnault, arXiv:1204.5682 (2012).

[5] Huaiming Guo, Shun-Qing Shen, Shiping Feng, *Phys. Rev. B* **86**, 085124 (2012).

[6] J.C. Budich, E. Ardonne, *Phys. Rev. B* **88**, 035139 (2013).

[7] Tian-Sheng Zeng, W. Zhu, D.N. Sheng, *Phys. Rev. B* **94**, 235139 (2016).

[8] B. Jaworowski, P. Kaczmarkiewicz, P. Potasz, A. Wójs, *Phys. Lett. A* **382**, 1419 (2018).

[9] S. Kourtis, T. Neupert, C. Chamon, C. Mudry, *Phys. Rev. Lett.* **112**, 126806 (2014).

[10] E.J. Bergholtz, J. Kailasvuori, E. Wikberg, T.H. Hansson, A. Karlhede, *Phys. Rev. B* **74**, 081308 (2006).

[11] M.J. Rice, E.J. Mele, Phys. *Rev. Lett.* **49**, 1455 (1982).

[12] B.A. Bernevig, N. Regnault, *Phys. Rev. B* **85**, 075128 (2012).

[13] E.M. Stoudenmire, S. White, Itensor, accessed 13 January 2018.